J. Mater. Environ. Sci. 7 (1) (2016) 299-309
ISSN : 2028-2508
CODEN: JMESC

The Influence of Some Pyrazole Derivatives on The Corrosion Behaviour of Mild Steel in 1M HCl Solution

S. El Arrouji[1], K. Ismaily Alaoui[1], A. Zerrouki[2], S. EL Kadiri[2], R. Touzani, Z. Rais[1], M. Filali Baba[1], M. Taleb[1*], A. Chetouani[2;3], A. Aouniti[2]

[1]*Laboratoire d'Ingénierie d'Electrochimie de Modélisation et Environnement, LIEME Faculté des sciences Dhar El Mahraz Fès Maroc »*

[2] *Laboratoire de Chimie Appliquée et environnement (LCAE-URAC18), Faculté des Sciences, 60000 Oujda, Morocco.*

[3]*Laboratoire de chimie physique, Centre Régionale des Métiers de l'Education et de Formation "CRMEF", Région de l'Orientale, Oujda, Morocco*

Received 12 Mar 2015, Revised 17 Nov 2015, Accepted 29 Nov 2015
**For correspondence: Email: mustaphataleb62@yahoo.fr*

Abstract
The inhibitive action of some pyrazole derivatives, namely N1, N1-bis (2-(bis ((3,5-dimethyl-1H-pyrazol-1-yl) methyl) amino)ethyl)-N2, N2-bis ((3,5-dimethyl-1H-pyrazol-1-yl) methyl) ethane-1,2-diamine: PAP and diethyl 1,1'-(((4-acetylphenyl) azanediyl) bis (methylene)) bis (5-methyl-1H-pyrazole-3-carboxylate): PAC against the corrosion of mild steel in 1 M HCl solution has been investigated using weight loss measurements, Tafel polarisation and electrochemical impedance spectroscopy (EIS) techniques. The experimental results obtained revealed that these compounds inhibited the steel corrosion in acid solution, the protection efficiency increased with increasing inhibitors concentration. The results obtained from the different corrosion evaluation techniques are in good agreement. Potentiodynamic polarisation studies clearly showed that PAP and PAC acted as mixed inhibitors affecting both cathodic and anodic corrosion currents. Adsorption of these inhibitors on steel surface obeyed to Langmuir adsorption isotherm. Thermodynamic data of adsorption showed that inhibition of steel corrosion in 1M HCl solution by pyrazole compounds is due to the formation of a chemisorbed film on the steel surface. SEM and EDX supported the adsorption conclusions.

Keywords: mild steel, pyrazole, corrosion, EIS, SEM

1. Introduction
The effects of corrosion in our daily lives are both direct, in that corrosion affects the useful service lives of our possessions, and indirect, in that producers and suppliers of goods and services incur corrosion costs, which they pass on to consumers.

Use of inhibitors is one of the most practical methods for protection against corrosion especially in acid solutions to prevent metal dissolution and acid utilization [1]. Recently, natural compounds are employed as inhibitors in order to develop new cleaning chemicals for green environment. Several studies have been published on the use of natural products as corrosion inhibitors in different media [2-10]. Most of the natural products are nontoxic, biodegradable and readily available in plenty.

The effect of organic compounds containing heteroatom on the corrosion behaviour of iron and steel in acidic solutions has been well documented and showed to be quite efficient to prevent corrosion [11-23] and in addition to heterocyclic compounds containing polar groups and π-electrons [24]. In wide part of our research programme, pyrazolic derivatives newly synthesized are tested as good corrosion inhibitors of aluminium, copper, lead, iron and steel [25-31]. The synthesis of pyrazolic compounds permit easily to obtain several compounds of which the molecular structure contains several heteroatoms and several substituents.

The aim of present work is to extend these investigations by studying the inhibitive properties of pyrazole on the corrosion of medium steel in 1 M HCl using electrochemical impedance spectroscopy method (EIS). The impedance spectra obtained from this study are analyzed to show the equivalent circuit that fits the corrosion data. The adsorption behaviour of these inhibitors compounds in 1 M HCl is discussed. Effects of temperature and isotherm adsorption are also determined by weight loss.

2. Experimental method

2.1. Inhibitors and material preparation

The tested inhibitors, namely N1, N1-bis (2-(bis ((3,5-dimethyl-1H-pyrazol-1-yl) methyl) amino)ethyl)-N2, N2-bis ((3,5-dimethyl-1H-pyrazol-1-yl) methyl) ethane-1,2-diamine : PAP and diethyl 1,1'-(((4-acetylphenyl) azanediyl) bis (methylene)) bis (5-methyl-1H-pyrazole-3-carboxylate) : APC were synthesized by similar procedures used to prepare their analogues described in the following references [32,33] for example. The molecular structures of these Pyrazole derivatives are shown in Fig. 1. The concentration range of Pyrazole derivatives employed was 10^{-6} to 10^{-3}M.

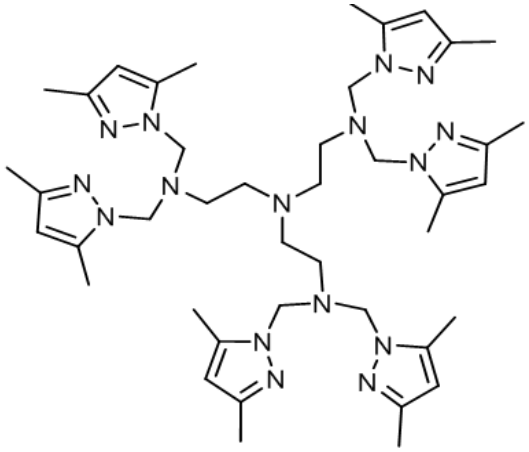

N1, N1-bis (2-(bis ((3,5-dimethyl-1H-pyrazol-1-yl) methyl) amino)ethyl)-N2, N2-bis((3,5-dimethyl-1H-pyrazol-1-yl) methyl) ethane-1,2-diamine : PAP

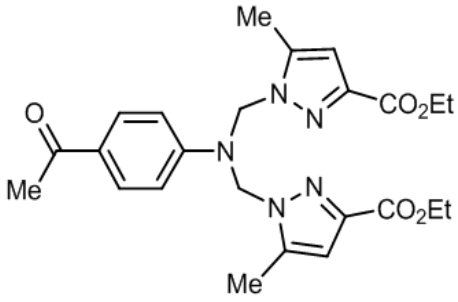

diethyl 1,1'-(((4-acetylphenyl) azanediyl) bis (methylene)) bis (5-methyl-1H-pyrazole-3-carboxylate) : APC

Figure 1.Chemical structure of new synthesized pyrazole derivatives.

The material used in this study was mild steel with chemical compositions 0.09 wt.% P, 0.38 wt.% Si, 0.01 wt.% Al, 0.05 wt.% Mn, 0.21 wt.% C, 0.05 wt.% S and balance iron. The mild steel samples were polished with silicon carbide emery (120, 600 and 1200) to produce a fine surface finishing, rinsed with distilled water, degreased in acetone. The solutions (1 M HCl) were prepared by dilution of an analytical reagent grade 37% HCl with doubly distilled water, degreased ultrasonically in ethanol.

2.2. Weight loss test

The gravimetric measurements were carried out in a cell equipped with a thermostated cooling condenser. The solution volume was 50 ml. The mild steel specimens used have a rectangular form (length = 2 cm, width = 1 cm, thickness = 0.2 cm). At the end of the tests, the specimens were carefully washed in acetone under ultrasound and then weighed. Weight loss allowed calculation of the mean corrosion rate in mg cm^{-2} h^{-1}.

2.3. Electrochemical techniques

Electrochemical measurements, including potentiodynamic polarization curves and electrochemical impedance spectroscopy (EIS) were performed in a three-electrode cell. Pure mild steel specimen was used as the working electrode, a platinum wire as the counter electrode and a saturated calomel electrode (SCEs) as the reference electrode. The specimens were embedded in epoxy resin leaving a working area of 1 cm^2. The working surface was subsequently ground with 1200 grit grinding papers, cleaned by distilled water and ethanol.

All tests were performed in continuously stirred conditions at room temperature; all tests were performed at 308 K. Potentiodynamic curves-polarization experiments were carried by Potentiostat Radiometer-analytical PGZ 100 and controlled with analysis software Voltamaster 4. The mild steel electrode was maintained at open circuit conditions (corrosion potential, E_{corr}) for 30 min and thereafter prepolarized at -800 mV for 10 min. After this scan, the potential was swept to anodic potentials. The anodic and cathodic polarization curves were recorded at scan rate of 1 mVs^{-1}. The EIS measurements were performed using a transfer function analyser (Voltalab PGZ 100), with a small amplitude a.c. signal (10 mV rms) over a frequency domain from 100 kHz to 10 MHz at 308 K with five points per decade. Computer programs automatically controlled the measurements

performed at rest potentials after 1 h of immersion at E_{corr}. The impedance diagrams were given in the Nyquist representation. In order to ensure reproducibility, all experiments were repeated three times.

2.4. Surface analysis

The surface morphology after immersion in 1 M HCl solution in the absence and presence of inhibitor was imaged using an environmental scanning electron microscope (FEI company quanta 200).

3. Results and discussion

3.1. Polarization measurements

Polarization curves were obtained for mild steel in 1 M HCl solution with and without inhibitor. Tafel lines which obtained in various concentrations of P1 and P2 solutions were shown in Fig. 2. This figure shows that the anodic and cathodic reactions are affected by the inhibitors. It means that the addition of P1 and P2 in the HCl solution reduces the anodic dissolution of steel and also retards the cathodic hydrogen evolution reaction. These results indicated that this inhibitor exhibits cathodic and anodic inhibition effects.

The respective kinetic parameters including corrosion current density (I_{corr}), corrosion potential (E_{corr}), cathodicTafel slope (β_c), anodic Tafel slope (β_a), and inhibition efficiency ($E\%$) are given in Table 1. The inhibition efficiency E% was calculated from I_{corr} using the following equation (1):

$$E\% = \frac{I_{corr} - I}{I_{corr}}$$

Where I_{corr} and I are the corrosion current density values in the absence and presence of PAP and APC, respectively.

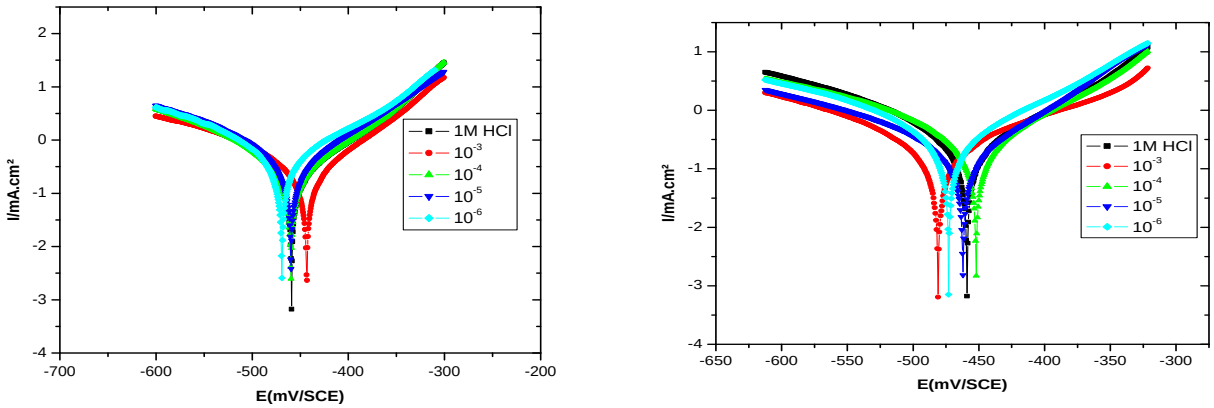

Figure 2: Polarization curves for mild steel in 1 M HCl in the absence and presence of different concentration of PAP and APC

It is illustrated from data of Table 1 that the addition of PAP and APC decreases corrosion current density. Also, it can be clearly seen that the inhibition efficiency of PAP and APC increases with inhibitor concentration, reaching a maximum value at 10^{-3}. This behavior shows that PAP and APC acts as effective inhibitor for the corrosion of mild steel in HCl media. The cathodic Tafel slope (βc) and the anodic Tafel slope (βa) of PAP and APC changed with inhibitor concentration. This observation suggests that the inhibitor molecules controlled the two reactions and adsorbed on the metal surface by blocking the active sites on the metal surface, retarding the corrosion reaction. Also, the presence of inhibitor results in a marked shift in the cathodic branches and to a lesser extent in the anodic branches on the polarization curves. These results indicated PAP and APC exhibits cathodic and anodic effects, which can be classified as mixed inhibitor in acid media.

3.2. Electrochemical impedance spectroscopy (EIS)

The R_{ct} values were used to calculate the inhibition efficiency E% according to the following equation 2:

$$E\% = \frac{R_{ct} - R^{\circ}_{ct(inh)}}{R_{ct}}$$

where R°_{ct} and R_{ct} are respectively the charge transfer resistance in the absence and the presence of PAP and APC, respectively.

Table 1.Polarization parameters and the corresponding inhibition efficiency for the corrosion of mild steel in 1 M HCl containing different concentrations of PAP and APC at 25 °C.

Inhibitors	Concentration	E_{corr} (mV/SCE)	I_{corr} (µA/cm²)	$\|\beta c\|$ (mV/decade)	E (%)
	HCl 1M	-521,3	1308,3	173.5	HCl 1M
	10^{-3}	-443.2	179.1	92.4	86
	10^{-4}	-459.8	192.1	79.5	85
PAP	10^{-5}	-459.6	284.8	92.2	78
	10^{-6}	-469.1	387.4	106.3	70
	10^{-3}	-480.9	186.2	111.1	85
	10^{-4}	-452.1	216.9	98.7	83
APC	10^{-5}	-462.1	339.6	183.6	74
	10^{-6}	472.9	599.7	186.2	54

Table 2. Impedance parameters of mild steel in 1M HCl containing different concentrations of the studied pyrazole compounds.

Inhbitors	Concentration mol L^{-1}	R_{ct} (Ω cm²)	F_{max} (Hz)	C_{dl} (µF cm^{-2})	E_R (%)
HCl 1M		21,63	55.3721	132	
	10^{-3}	143,4	7,9365	76	85
PAP	10^{-4}	100,6	15,823	95	82
	10^{-5}	55	15,823	102	79
	10^{-6}	74	4	126	72
	10^{-3}	132	15,823	87	84
APC	10^{-4}	118	15,823	95	80
	10^{-5}	105	15,823	111	74
	10^{-6}	81	15,823	130	62

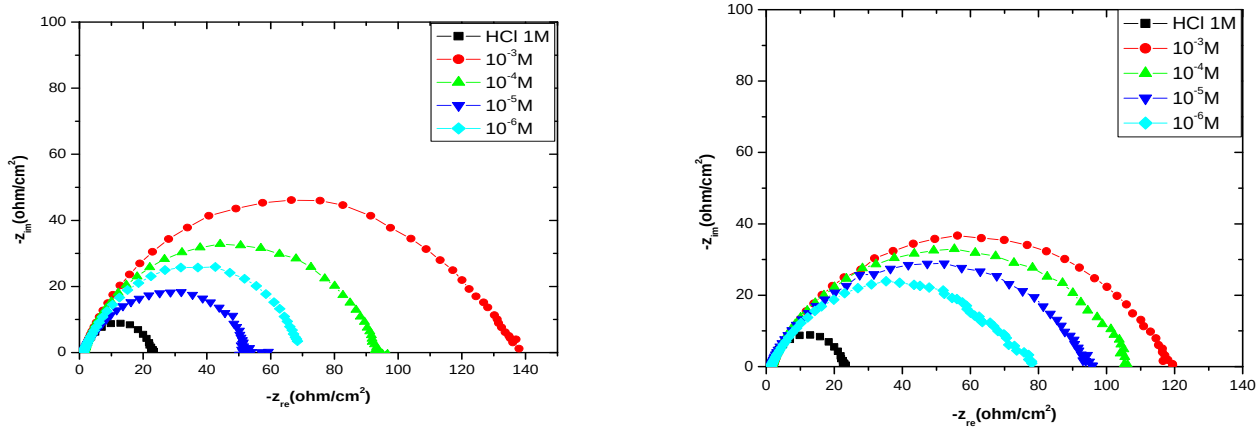

Figure 3. Nyquist diagrams for mild steel in 1M HCl without and with different concentrations of the undertaken inhibitors PAP and APC.

From Table 2, it is clear that the addition of the inhibitors decreases the double layer capacitance and increases the charge transfer resistance; as consequence, a large diameter of the semicircle is observed in Nyquist plots.

The decrease in C_{dl} could be attributed to the adsorption of the inhibitors on the electrode surface, forming protective adsorption layers. These findings indicate that, PAP and APC inhibit mild steel corrosion by adsorption. Furthermore, the magnitude of C_{dl} decreases with increasing inhibitors concentrations. This situation can be interpreted as a result of increase in the surface coverage by PAP and APC, which led to an increase in the inhibiting efficiency (Table 2). The thickness of the protective layer, d, is related to C_{dl} by the following Equation 3:

$$\delta = \frac{\varepsilon\varepsilon_0}{C_{dl}} S$$

Where, ε_0, ε, and S stand, respectively, for the vacuum dielectric constant (ε_0 = 8.854×10^{-14} F cm $^{-1}$), the relative dielectric constant, and the surface area. This decrease in C_{dl}, which can result from a decrease in local dielectric constant and/or an increase in the thickness of the electrical double layer, suggested that PAP and APC function by adsorption on the medium steel at the metal/solution interface.

3.3. Effect of temperature:

The change of the corrosion process rate with the temperature increase was studied in 1 M HCl in the absence and in the presence of inhibitor by weight measurements, in the temperature range 308– 353 K, are shown in Table 3.

Table 3. Influence of temperature on the corrosion rate and inhibition efficiency of mild steel in 1 M HCl at different concentrations of PAP and APC

		PAP		APC	
Temperature (K)	Concentrations (M)	W_{corr} (mg/cm².h)	IE_W %	W_{corr} (mg/cm².h)	IE_W %
308	0	0.86		0.86	
	10^{-3}	0.12	86	0.14	84
	10^{-4}	0.16	81	0.19	78
	10^{-5}	0.36	58	0.26	70
	10^{-6}	0.57	34	0.33	62
313	0	1.3		1.3	
	10^{-3}	0.18	86	0.25	81
	10^{-4}	0.3	77	0.36	72
	10^{-5}	0.58	55	0.49	62
	10^{-6}	0.98	25	0.57	56
323	0	3.47		3.47	
	10^{-3}	0.55	84	0.71	79
	10^{-4}	0.67	81	0.98	72
	10^{-5}	1.14	67	1.48	57
	10^{-6}	1.84	47	1.58	54
333	0	6.72		6.72	
	10^{-3}	1.13	83	1.59	76
	10^{-4}	1.69	75	1.92	71
	10^{-5}	1.86	72	3.15	53
	10^{-6}	2.95	56	3.77	44

The corrosion rates increase with rise of temperature both in uninhibited and inhibited solutions. Moreover, the mild steel corrosion increased more rapidly with temperature in the presence of PAP than with APC. Apparently, the results obtained postulate that the inhibitor function through adsorption on the metal surface by the blocking the active sites to form a screen onto the mild steel surface from acidic solution. As the temperature increases, we notice the desorption rate manifests parallel to that of adsorption [34]**;** the surface becomes less protected and then the inhibitor gradually loss its effectiveness.

We were interested in the activation energy of the corrosion process and the kinetic parameters of the inhibitors adsorption. This was accomplished by investigating the temperature dependence of the corrosion current,

obtained using weight measurement method. The corrosion reaction can be regarded as an Arrhenius-type process, the rate is given by the following equation 4:

$$W = K\ exp\left(-\frac{Ea}{RT}\right)$$

Where E_a is the apparent activation corrosion energy, T is the absolute temperature, A is the Arrhenius pre-exponential constant and R is the universal gas constant. This equation can be used to calculate theE_a values of the corrosion reaction without and with inhibitors. The logarithm of the corrosion current density versus 10^3/T and the activation energy (E_a) values can be calculated from the Arrhenius slope (Fig. 4). The calculated values of the apparent activation corrosion energy in the absence and presence of P1 and P2 are listed in Table 4.
All the linear regression coefficients were close to one. In 1 M HCl, the addition of Pyrazole compounds leads to an increase in the apparent activation energy to values greater than that of the uninhibited solution. Consequently, the rate of corrosion decreases due to the formation of the metal complex layer [35]. Szauer and Brand explained that the increase in activation energy can be attributed to an appreciable decrease in the adsorption of the inhibitor on the mild steel surface with the increase in temperature.

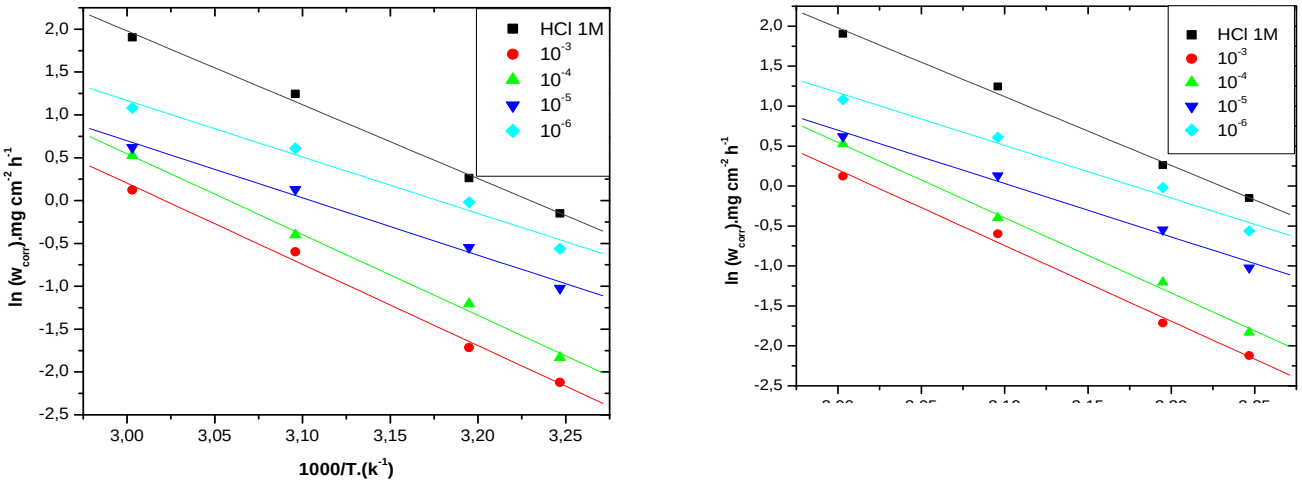

Figure 4. Arrhenius plots of mild steel in 1 M HCl at different concentrations of PAP and APC

When there is reduction in the adsorption, a greater desorption of the inhibitory molecules occurs because these two opposite processes are in equilibrium. Because of this most important desorption of the inhibitor molecules at higher temperatures, a greater mild steel surface is in contact with aggressive environment, involving higher corrosion rates with increasing temperature[36].

Equation 5:

$$W = \frac{RT}{Nh}\exp\left(\frac{\Delta S°a}{R}\right)\exp\left(\frac{\Delta H°a}{RT}\right)$$

Where h is Planck's constant, N is Avagadro's number, ΔS_a is the entropy of activation and ΔH_a is the enthalpy of activation. Fig. 5 shows a plot of ln ($W_{corr}.T^{-1}$). 10^3. T^{-1}. Straight lines are obtained with a slope of $\Delta H_a/R$ and an intercept of ln ($R/Nh + \Delta S_a/R$) from which the values of ΔS_a and ΔH_a are calculated and are given in Table 4. The values of the entropy of activation ΔS_a given in Table 4 are negative.

3.4. Adsorption isotherm

C_{inh}/θ versus C_{inh} yield straight lines with nearly unit slope and the best fits are obtained with Langumir adsorption isotherm as presented in Fig. 6. It is found that all the linear correlation coefficients are very closed to 1.00, clearly proving that the adsorption of these pyrazole derivatives from 1 M HCl solution on the mild steel obeys the Langmuir adsorption isotherm.

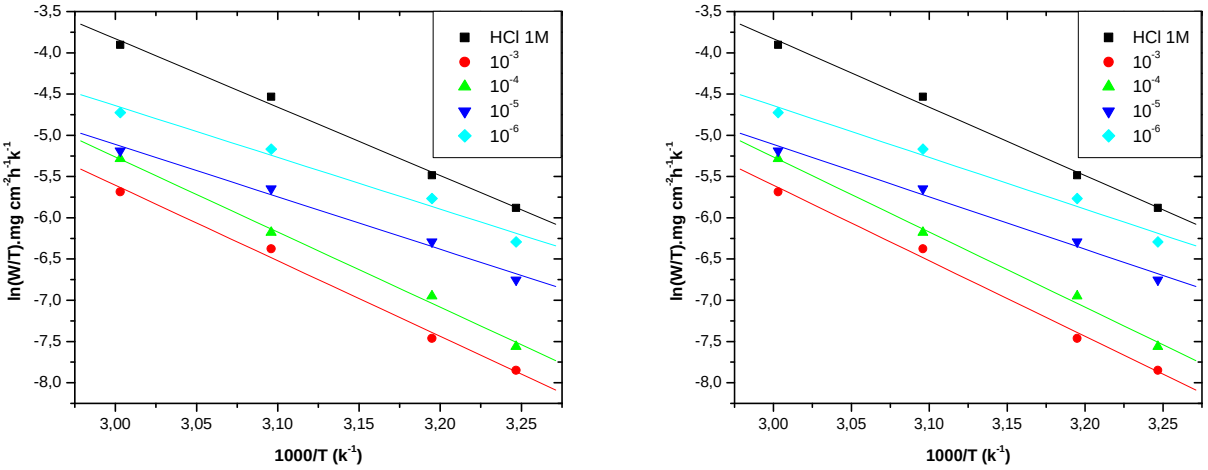

Figure 5. The relationship between ln (W/T) and 1/T for mild steel at different concentrations of PAP and APC

Table 4. Activation parameters of the dissolution reaction of mild steel in 1 M HCl in the absence and presence different concentration of PAP and APC

Concentration (M)	E_a (KJ.mol^{-1})	ΔH° (kJ.mol^{-1})	ΔS° (J.mol^{-1}.K^{1})	E_a (KJ.mol^{-1})	ΔH° (kJ.mol^{-1})	ΔS° (J.mol^{-1}.K^{-1})
HCl (1M)	71,61	68,95	-22,52	71,61	68,95	-22,52
10^{-3}	78,76	76,10	-15,85	83,11	80,45	0,024
10^{-4}	78,36	75,69	-14,20	78,76	76,10	-11,15
10^{-5}	55,48	52,82	-81,58	85,45	82,78	12,98
10^{-6}	54,79	52,13	-79,74	83,23	80,57	7,36

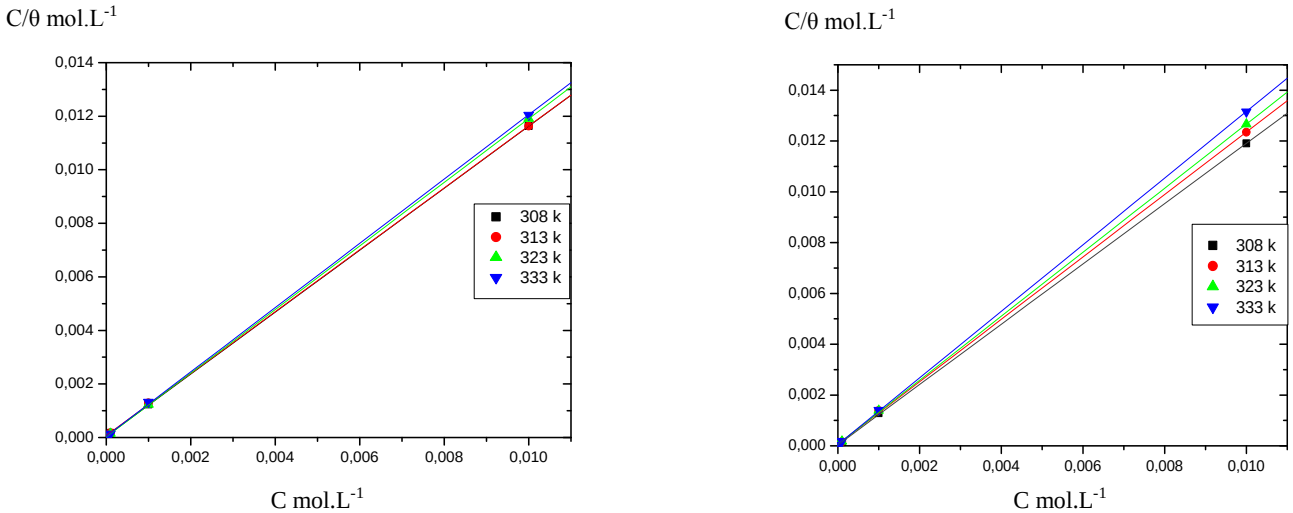

Figure 6. Langmuir adsorption plots for mild steel in 1 M HCl containing different concentrations of pyrazole derivatives.

From the intercepts of the straight lines C_{inh}/θaxis, K value can be calculated. The constant of adsorption, K, is related to the standard free energy of adsorption, $\Delta G_{ads}°$, by the following equation:

$$K = \frac{1}{55.5} \exp\left(-\frac{\Delta G°ads}{RT}\right)$$

Table 5. Slope, regression coefficient and free enthalpy of adsorption of pyrazole compounds on mild steel in 1M HCl at different temperature.

Temperature (K)	R^2	Slope	$\Delta G_{ads}°$ (kJ.mol^{-1})	R^2	Slope	$\Delta G_{ads}°$ (kJ.mol^{-1})
308	0.9999	1.1	35.7	0.9999	1.1	35.5
313	0.9999	1.1	35.1	0.9999	1.2	35.8
323	0.9999	1.1	38.9	0.9999	1.2	36.7
333	0.9999	1.2	38.6	0.9999	1.1	39.2

Where *R* is the universal gas constant and T is the absolute temperature. The calculated standard free energy of adsorption. The negative values of $\Delta G_{ads}°$ ensure the spontaneity of the adsorption process and stability of the adsorbed layer on the steel surface. Its well known that values of $-\Delta G_{ads}°$ of the order of 20 kJ mol^{-1} or lower indicate a physisorption; those of order of 40 kJ mol^{-1} or higher involve charge sharing or transfer from the inhibitor molecules to the metal surface to form a coordinate type of bond (chemisorption) [38-42]. The calculated $\Delta G_{ads}°$ value in the case of Pyrazole indicates, therefore, that the adsorption mechanism of the investigated PAP and APC on the mild steel surface in 1 M HCl solution is typical of chemisorption.

3.5. Surface analysis

SEM micrographs, obtained from mild steel surface specimens immersed in 1 M HCl solution for 6 h in the absence and presence of 10^{-3} of pyrazole compounds, are shown in Fig. 9. Fig. 9a indicates the finely polished characteristic surface of mild steel and shows some scratches due to polishing. Fig. 9b reveals that the surface is highly corroded in the absence of inhibitor due to the direct attack of aggressive acids. By the comparison of SEM images at the same magnification (Fig. 9c and d), it appears that mild steel surface is free from corrosion in HCl solution. This is due to the formation of an adsorbed film of PAP and APC on the surface. This shows that the inhibitor inhibits corrosion of mild steel in 1 M HCl solution.

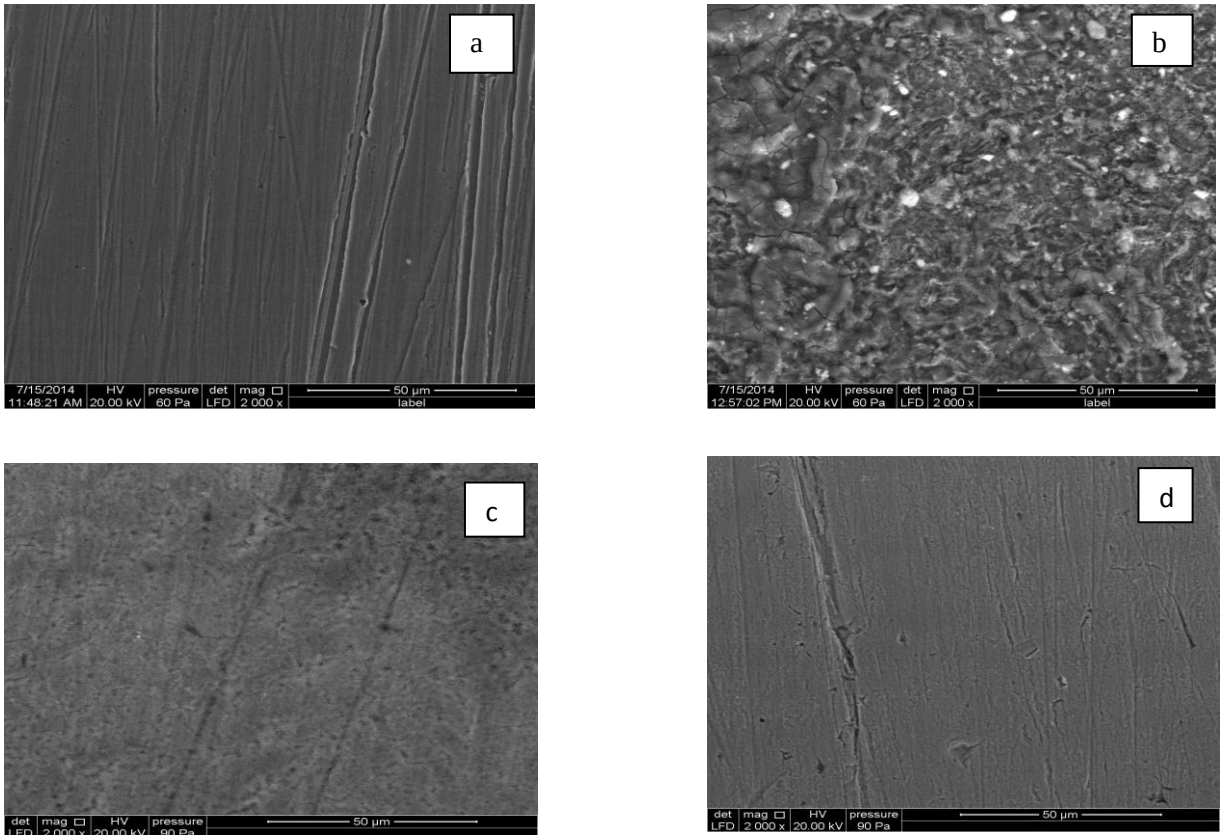

Figure 9. SEM micrographs of mild steel (a) polished, (b) after immersion in 1 M HCl without inhibitors, (c) after immersion in 1 M HCl solution containing 10^{-3} of PAP and (d) after immersion in 1M HCl solution containing 10^{-3} of APC.

EDX spectra survey was used to determine which elements are present on the mild steel surface before and after exposure to the inhibitors solution. Indeed, after mild steel has been immersed in the absence and presence of PAP and APC for 6 h, its surface film composition was determined by EDX. The results are displayed in figure and the Table 4. Comparison of the two spectra shows the formation of iron oxides resulting from corrosion of steel in 1 M HCl solution, as evidenced by the appearance of the oxygen peak on the EDX spectrum of steel in HCl 1 M. After 6 h of immersion, the EDX spectra showed an additional signal for the existence of Cl element on the surface. Moreover, in inhibited solution, the EDX spectra showed an additional signal for the existence of N element (due to the nitrogen atoms of the inhibitors) [43]. In addition, the O and Cl signals are significantly reduced. These data show the adsorption of PAP and APC on the surface of the steel.

a

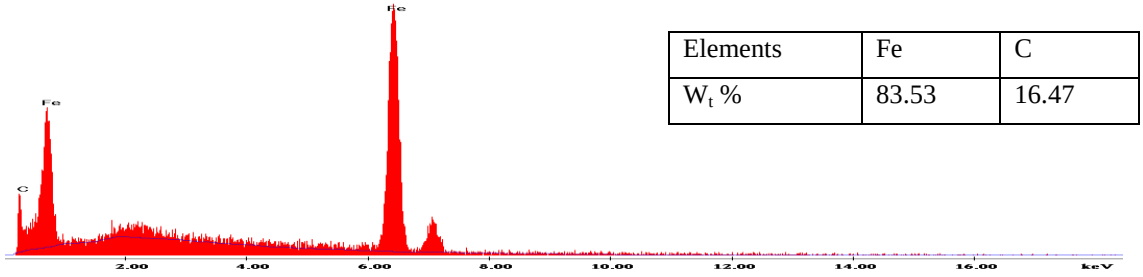

Elements	Fe	C
W_t %	83.53	16.47

b

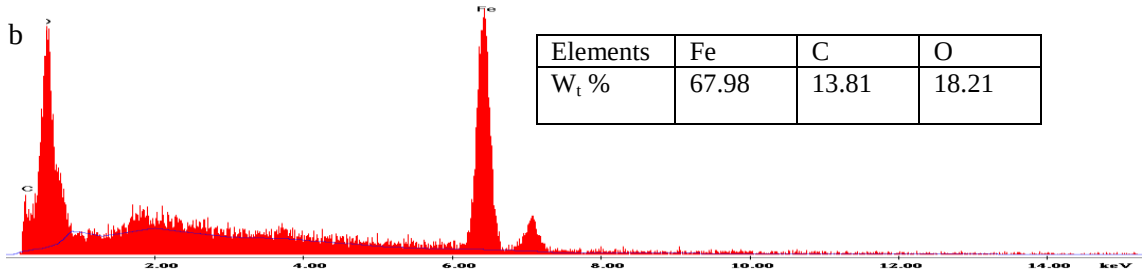

Elements	Fe	C	O
W_t %	67.98	13.81	18.21

c

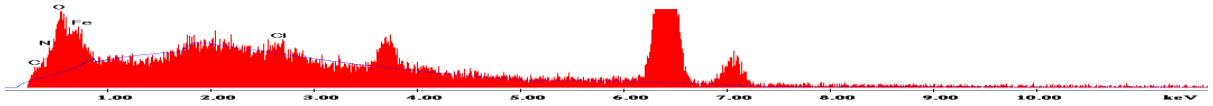

Elements	Fe	C	O	N	Cl
W_t %	89.01	0	6.39	3.48	1.12

d

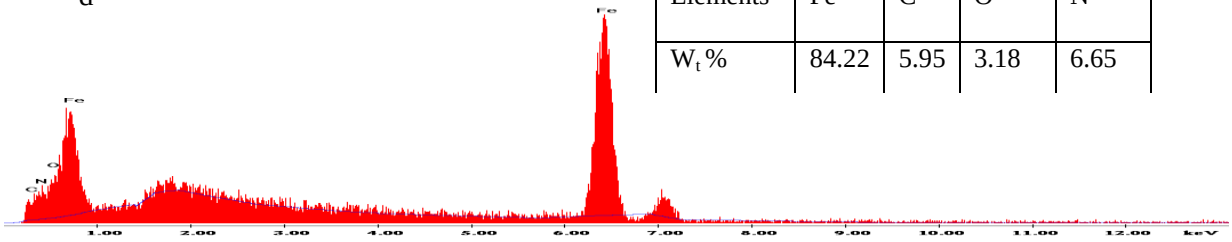

Elements	Fe	C	O	N
W_t %	84.22	5.95	3.18	6.65

Figure 10. Percentage in mass obtained from EDX analyzes of the different elements composing the mild steel surface, after immersion in 1 M HCl without inhibitors, (c) after immersion in 1 M HCl solution containing 10^{-3} of PAP and (d) after immersion in 1M HCl solution containing 10^{-3} of APC.

Conclusions

From the above results and discussion, the following conclusions are drawn:
Pyrazole compounds inhibit the corrosion of mild steel in 1 M HCl. The inhibition efficiency increases by increasing the inhibitor concentration.
The results obtained from weight loss measurements, polarisation curves and ac impedance study are in reasonable agreement.
The electrochemical parameters indicated that both the tested pyrazoles derivatives acted essentially as mixed-type inhibitors.
The adsorption process for pyrazole derivatives on the steel surface obeys to the Langmuir isotherm equation in 1 M HCl solution.
SEM study confirmed the formation of protective layer over the steel surface by the green inhibitor.

References

1. Sykes Silver J., Jubilee review 25 years of progress in electrochemical methods *British Corrosion Journal*, 25 (1990) 175–183
2. Satapathy A.K., Gunasekaran G., Sahoo S.C., Kumar Amit, Rodrigues P.V., *Corros. Sci.*, 51 (2009) 2848–2856
3. Abdel-Gaber A.M., Khamis E., Abo-ElDahab H., Adeel Sh., *Mater. Chem. Phys*., 109 (2008) 297–305
4. Abdel-Gaber A.M., *Int. J. Appl. Chem*., 3 (2007) 161–167
5. Saratha R., Vasudha V.G., *J. Chem*., 6 (2009) 1003–1008
6. Abiola O.K., James A.O., *Corros. Sci*., 52 (2010) 661–664
7. Abdel-Gaber A.M., Abd-El-Nabey B.A., Saadawy M.,*Corros. Sci*., 51 (2009) 1038–1042
8. da Rocha J.C., Ponciano Gomes N.D.C., D'Elia E., *Corros. Sci.*, 52 (2010) 2341–2348
9. Kanojia R., Singh G., *Surf. Eng*., 21 (2005) 180–186
10. Ostovari A., Hoseinieh S.M., Peikari M., Shadizadeh S.R., Hashemi S.J., *Corros. Sci*., 51 (2009) 1935–1949
11. Pillali C., Narayan R., *Corros. Sci*., 23 (1983) 151
12. Growcock, Lopp V.R., *Corros. Sci*., 28 (1988) 397
13. Bentiss F., Traisnel M., Lagrenée M., *Corros. Sci*., 42 (2000) 127
14. Bekkouch K., Aouniti A., Hammouti B., Kertit S., *J. Chim. Phys*., 96 (1999) 838
15. Kertit S., Bekkouch K., Hammouti B., *Rev. Metall*. (Paris), 97 (1998) 251
16. Bouzidi D., Kertit S., Hammouti B., Brighli M., *J. Electrochem. Soc. India*, 46 (1997) 23
17. Kertit S., Hammouti B., Taleb M., Brighli M., *Bull. Electrochem*., 13 (1997) 241
18. Hammouti B., Melhaoui A., Kertit S., *Bull. Electrochem*., 13 (1997) 97
19. Chetouani A., Aouniti A., Hammouti B., Benchat N., Benhadda T., Kertit S., *Corros. Sci.*, 45 (2003) 1675
20. Chetouani A., Hammouti B., Aouniti A., Benchat N., Benhadda T., *Progr. Org. Coat*., 45 (2002) 373
21. Muralidharan S., Chandrasekar R., Kiyer S.V., *Proc. Indian Acad. Sci. (Chem. Sci.)*, 112 (2000) 127
22. Bouklah M., Bouyanzer A., Benkaddour M., Hammouti B., Oulmidi M.,Aouniti A., *Bull. Electrochem*., 19 (2003) 483
23. Dean S.W., Derby Jr. R., Vondembussche G.T. *Mater. Perform*. 20 (1981) 47
24. Riggs O.L., *Jr.Corrosion Inhibitors* (2nd ed.)C.C. Nathan, Houston, TX (1973)
25. Touhami F., Aouniti A., Kertit S., Abed Y., Hammouti B., Ramdani A., El- Kacemi K., *Corros. Sci.*, 42 (2000) 929
26. Touhami F., Hammouti B., Aouniti A., Kertit S., *Ann. Chim. Sci. Mater.*, 24 (1999) 581
27. El-Ouafi A., Hammouti B., Oudda H., Kertit S., Touzani R., Ramdani A., *Anti-corros. Meth. Mater*., 49 (2002) 199
28. Dafali A., Hammouti B., Touzani R., Kertit S., Ramdani A., El Kacemi K., *Anti-corros. Meth. Mater*., 49 (2002) 96
29. Bouklah M., Attayibat A., Hammouti B., Ramdani A., Radi S., Benkaddour M., *Appl. Surf. Sci.*, 240 (2005) 341

30. Salghi R., Bazzi L., Hammouti B., Zine E., Kertit S., El Issami S., Ait Eddi E., *Bull. Electrochem.*, 17 (2001) 429
31. Aouniti A., Hammouti B., Brighli M., Kertit S., Berhili F., El-Kadiri S., Ramdani A., *J. Chim. Phys.*, 93 (1996) 1261
32. Bouabdallah I., Touzani R., Zidane I., Ramdani A., *Catalysis communication*., 8 (2007) 707-712.
33. Daoudi M., Ben Larbi N., benjelloun D., Kerbal A., Launay J.P., Bonvoisin J., Jaud J., Mimouni M., and T. Ben Hadda , *Molecules.*, 7(2002) 690-696.
34. Zarrouk A., Warad I., Hammouti B., Dafali A, Al-Deyab S.S., Benchat N., *Int. J. Electrochem. Sci*., 5 (2010) 1516 – 1526
35. Bammou L., Belkhaouda M., Salghi R., Benali O., Zarrouk A., Al-Deyab S.S., Warad I., Zarrok H., Hammouti B., *Int. J. Electrochem. Sci.*, 9 (2014) 1506–1521
36. Szauer T., Brand A., *Electrochim. Acta*, 26 (1981) 1253–1256
37. Agrawal R., Namboodhiri T.K.G., *Corros. Sci.*, 30 (1990) 37
38. Donahue F.M., Nobe K., *J. Electrochem. Soc*., 112 (1965) 886
39. El Ouadi Y., Bouyanzer A., Majidi L., Elmsellem H., Cherrak K., Elyoussfi A., Hammouti B., Costa J., *Ar. J. Chem. Environ. Res.* 1 (2014) 49-56
40. Khamis E., Belluci F., Latanision R.M., El-Ashry E.S.H., *Corrosion*, 47 (1991) 677
41. Anejjar A., Salghi R., Jodeh S., Karzazi Y., Warad I., Dassanayake R., Hamed O., Zarouk A., Hammouti B., *Maghr. J. pure Appl. Sci.* 1 (2015) 25-38
42. Tebbji K., Bouabdellah I., Aouniti A., Hammouti B., Oudda H., Benkaddour M., Ramdani A., *Mater. Let.* 61 (2007) 799-804
43. Toumiat K., Guibadj A., Taouti B. M., Lanez T., *Mor. J. Chem.* 3 (2015) 809-823